PERGAMON

Electrochimica Acta 46 (2001) 1493–1498

ELECTROCHIMICA Acta

www.elsevier.nl/locate/electacta

Structure and conductivity in polydioxolane/$LiCF_3SO_3$ electrolytes

R.A. Silva [a], G. Goulart Silva [b,*], C.A. Furtado [c], R.L. Moreira [a], M.A. Pimenta [a]

[a] *Departamento de Física, Universidade Federal de Minas Gerais, C.P. 702, Belo Horizonte, MG 31270-901, Brazil*
[b] *Departamento de Química, Universidade Federal de Minas Gerais, C.P. 702, Belo Horizonte, MG 31270-901, Brazil*
[c] *Centro de Desenvolvimento da Tecnologia Nuclear — CDTN/CNEN, Belo Horizonte, MG, Brazil*

Received 12 July 2000; received in revised form 20 October 2000

Abstract

Thermal transition (T_g and T_m), ionic association and ionic conductivity have been measured as a function of $LiCF_3SO_3$ concentration in polydioxolane $(–CH_2OCH_2CH_2O–)_n$-based electrolytes. DSC and X-ray diffraction measurements were performed on samples with wt% between 2 and 58 wt% (n = O:Li ratio between 207 and 3), as well as on the pure polymer. Ionic association in the electrolytes was investigated by micro-Raman spectroscopy at room temperature. Conductivity isotherms at 300, 323 and 345 K were obtained. It was found that: (a) T_g increases from -69 to -44°C with increasing salt concentration; (b) the electrolyte is completely amorphous between 22 and 30 wt%; (c) the relative areas of the Raman peaks associated with different ionic species indicate the appearance of a new peak for a crystalline polymer/salt complex, also identified by the X-ray diffractograms; and (d) the ionic conductivity at 300 K shows a large maximum value of 7×10^{-5} S cm^{-1} between 12 and 48 wt%.

Keywords: Polydioxolane; DSC; X-ray; Micro-Raman; Conductivity

1. Introduction

Polymer electrolytes based on linear polydioxolane (PDXL, repeat unit $[CH_2OCH_2CH_2O]$) have been presented as an alternative host for the study of ionic conductors and their applications [1–4]. The various electrolytes based on poly(ethylene oxide) (PEO, repeat unit $[CH_2CH_2O]$), linear-semicrystalline, modified-amorphous and networks, are the most explored materials for salt dissolution for use in electrochemical devices as well as for fundamental studies [5,6]. However, the search for new systems is constant in the polymer electrolyte field [7,8]. The mechanism of ionic transport and its intriguing structural features have inspired a great research effort [9].

Linear PDXL (Mn = 30 000) complexed with $LiClO_4$ (n = (O:Li) = 8–16) showed an electrical conductivity behavior similar to that of semicrystalline PEO electrolytes [2]. Conductivities lower than 10^{-7} S cm^{-1} at room temperature and of approximately 10^{-3} S cm^{-1} at 100°C were measured. It was also shown [2] that the plasticizer salt $Li(CF_3SO_2)_2N$ [10] allows the preparation of amorphous PDXL/salt samples with conductivities higher than 5×10^{-6} S cm^{-1} at room temperature. Alamgir et al. [4] reported higher conductivities at room temperature for PDXL/$LiClO_4$ (4×10^{-6} S cm^{-1}). However, these authors' results may be associated with the low molar mass of their PDXL (not reported), which prevents crystallization.

* Corresponding author. Fax: +55-31-499-5700.
E-mail address: glaura@dedalus.lcc.ufmg.br (G. Goulart Silva).

0013-4686/01/$ - see front matter

In a previous work we performed a micro-Raman study of PDXL/$MClO_4$ systems (M = Li and Na) [3]; our results also presented similar data in relation to Raman studies of PEO and poly(propylene oxide) (PPO) electrolytes [11]. The totally symmetric stretching mode (ν_1) of ClO_4^- anion was fitted with an increased number of Lorentzian lines between the diluted systems up to the concentrations near $n = 3$. The presence of material heterogeneities and salt microprecipitation for $n = 3$ was also observed.

PDXL is an interesting matrix to compare with other well studied polyether systems. The repeat unit still contains one C–C–O sequence interspersed by a C–O sequence. The crystalline unit cell presents the dimensions $a = 9.07$ Å, $b = 7.79$ Å and $c = 9.85$ Å [12], while for the PEO unit cell the dimensions are $a = 8.16$ Å, $b = 12.99$ Å and $c = 19.30$ Å [13], the c direction being parallel to the helix axes. Therefore, in relation to PEO, PDXL presents a more compact helical structure. Recently, it was proposed that the amorphous phase (where the ionic transport occurs) shows a similar short-range helical arrangement [14]. Consequently, we can expect ionic conductors prepared with a PDXL host matrix to have different conductivity and structural features in comparison to PEO-based electrolytes.

In this study, we attempt to investigate further the behavior of PDXL in relation to ionic transport processes, interionic interactions and crystal/amorphous structure. For this electrical conductivity, thermal analysis, Raman spectroscopy and X-ray diffraction measurements were performed on PDXL/$LiCF_3SO_3$ electrolytes. The compositions ranged from 2 to 58 wt% of salt (ether oxygen to lithium ratio [O:Li] from 207 to 3).

2. Experimental

The polymerization of 1,3-dioxolane (Jansen) was carried out in a glove box under Ar atmosphere using benzoyl cation as initiator, as described elsewhere [2].

GPC measurements were carried out using a Waters 590 GPC equipped with a differential refractometer, Waters 410. The solvent (THF) was eluted (1.2 ml min^{-1}) through three Ultrastyragel columns (500, 10^3 and 10^4 Å). GPC results were: $M_w = 10\,000$ and polydispersity = 1.6.

Solutions in the concentration range between 2 and 58 wt% of $LiCF_3SO_3$ (Aldrich) were prepared by dissolving both salt and polymer in acetonitrile (Quimis). Films were obtained by casting these solutions in Petri dishes, removing the solvent slowly at ambient pressure, followed by vacuum ($\sim 10^{-1}$ bar) evaporation for several days at 60°C. The samples were stored in a desiccator.

TG analysis was performed using a TA Instruments SDT 2960 simultaneous DTA–TGA instrument with a scan rate of 10°C min^{-1} up to 600°C, under N_2 atmosphere. TG data were used to guarantee that the DSC thermal events, which will be shown later, are phase transitions rather than being associated with any loss of volatiles. The pure polymer decomposed in a single step beginning at 360°C. The introduction of the salt promoted the creation of a second stage, which reflected the salt/polymer complex degradation beginning at approximately 170°C.

DSC measurements were carried out with a TA Instruments 2920 DSC in two scanning experiments: 25–100°C and −100 to 100°C, at heating rates of 10°C min^{-1}, under He atmosphere (70 ml min^{-1}). Samples with masses of approximately 5 mg were sealed in aluminum DSC pans. Transition (T_g, T_m) values are quoted on the second heating scan as the extrapolated onset.

X-ray diffraction measurements were performed using a RIGAKU diffractometer with the CuK_α at room temperature. The scan rate for 2θ was 8° min^{-1} in the 2θ range of 4–70°.

Raman spectra were recorded in a triple monochromator spectrometer (Dilor XY) equipped with a multiarray (Gold) and CCD detectors. A microscope (Olympus BH-2) was coupled to the spectrometer, allowing a Raman analysis with spatial resolution of about 1 μm (micro-Raman technique). An argon laser was used operating in the green line ($\lambda = 514.5$ nm) with a power of 50 mW.

The total ionic conductivity was measured with a Hewlett–Packard 4192A electrochemical impedance spectrometer. The films were sandwiched by two stainless steel electrodes. Measurements were performed in the range of 300–365 K using the frequency range of 100 Hz to 5 MHz.

3. Results and discussion

3.1. DSC and X-ray measurements

DSC typical curves for PDXL/$LiCF_3SO_3$ are shown in Fig. 1 and the values of T_g, T_m and ΔH_m are assembled in Table 1.

Pure PDXL presents a low T_g (onset) of −69°C and a melting temperature (onset) of 50°C. Crystallization studies of PDXL have demonstrated the existence of two phases associated with different crystalline structures [15]. The T_m of 50°C is related to the so-called Phase II, which typically has a spherulitic morphology. This is the phase observed in DSC curves after a first heating, which erases the thermal history of the samples.

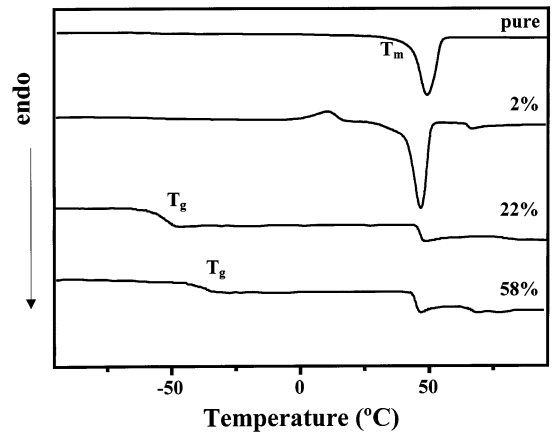

Fig. 1. DSC typical curves (second heating run) for pure PDXL and PDXL/$LiCF_3SO_3$ systems. Compositions are indicated in the figure.

Table 1
DSC results for PDXL/$LiCF_3SO_3$

Salt (wt%)	$T_g \pm 2$ (°C)	$T_m \pm 1$ (°C)	ΔH_m (J g^{-1})
0	−69	50	107
2	−52	48	118
5	−54	50	91
12	−63	33	62
22	−60		
30	−53		
46	−51		
58	−44		

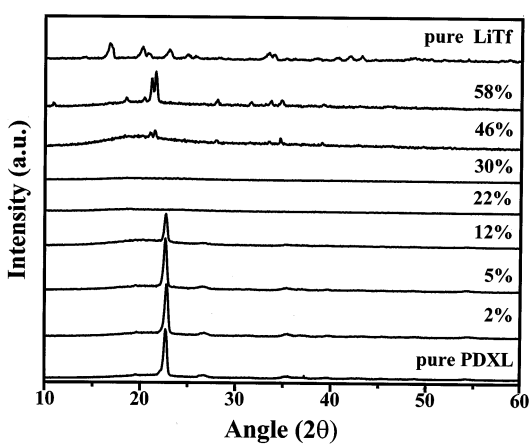

Fig. 2. X-ray diffractograms for pure PDXL, pure $LiCF_3SO_3$ and PDXL/$LiCF_3SO_3$ systems. Compositions are indicated in the figure.

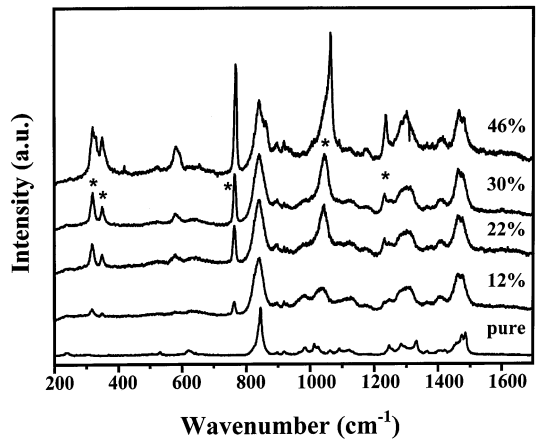

Fig. 3. Raman spectra for pure PDXL and PDXL/$LiCF_3SO_3$ systems. Compositions are indicated in the figure.

A similar kind of crystalline phase is observed for samples with 2 and 5 wt% of salt, whose T_m's and heat of fusion are approximately the same found for pure PDXL (considering salt concentration). The 12 wt% salt presents a decrease in T_m (Table 1), which indicates that the microstructure can no more be organized in spherulites of the same size, i.e. the $LiCF_3SO_3$ interactions disturb the PDXL crystals. This interpretation is corroborated by the X-ray diffractograms shown in Fig. 2. Between the pure PDXL and the 12 wt% of salt electrolyte the narrow Bragg peaks in Fig. 2 at the same 2θ angle indicate that a similar crystalline structure is present. Fig. 2 shows that the samples with 22 and 30 wt% salt are completely amorphous. The compositions of PDXL/$LiCF_3SO_3$ with 46 and 58 wt% salt present a growing of narrow Bragg peaks, which do not correspond either to the pure polymer or to the pure $LiCF_3SO_3$ salt. These diffractograms show the presence of an interesting crystalline complex between polymer/salt at 46 and 58 wt% ($n = 3$).

As it was shown by the DSC data in Table 1, no melting peak is observed between 22 and 58 wt% salt electrolytes. This behavior may be associated to a high melting point of the polymer/salt complexes, at least higher than 100°C.

In Table 1 is interesting to note the variations of T_g data. Between the pure PDXL and the first two electrolytes (2 and 5 wt%) an abrupt increase in T_g is observed. On the other hand, an almost linear increase in T_g is obtained for samples 0, 12, 22, 30, 46 and 58 wt%, and this behavior is often found for electrolyte systems [16,17]. In the case of samples with 2 and 5 wt% salt one observes a high degree of crystallinity, and the T_g values are also higher than expected. Therefore, these T_g values might be explained on the basis of a more constraint amorphous phase.

Table 2
Raman bands and assignments for $LiCF_3SO_3$

Bands (cm^{-1})	Assignments [18]
323	ν(C–S)
348	$E(SO_3)$
522	$E(\delta_d CF_3)$
579	$(\delta_s SO_3)$
773	$(\delta_s CF_3)$-solution
776	$(\delta_s CF_3)$
1040	$\nu(SO_3)$-solution
1057	$\nu(SO_3)$-solution
1071	$\nu(SO_3)$-crystal
1234	$(\nu_s CF_3)$
1246	$(\nu_{as} SO_3)$

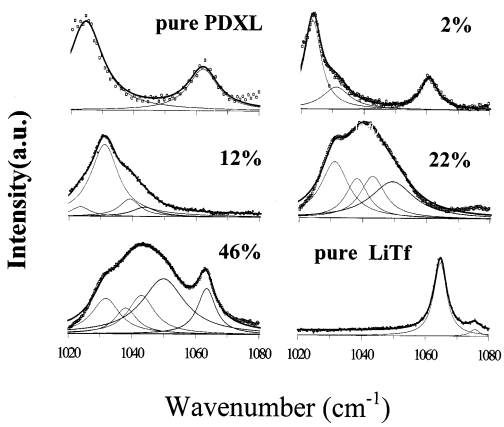

Fig. 4. Raman spectra in the region of the $\nu(SO_3)$ mode for pure PDXL, pure $LiCF_3SO_3$ and PDXL/$LiCF_3SO_3$ systems fitted by a sum of Lorentzian lines. Compositions are indicated in the figure.

3.2. Raman spectroscopy study

Fig. 3 shows micro-Raman spectra for PDXL/$LiCF_3SO_3$ samples in the region from 200 to 1700 cm^{-1}. Between the pure PDXL and the 46 wt% salt the growth of the bands associated to the anion $CF_3SO_3^-$ is observed. The most intense bands are indicated by (*) in Fig. 3. Table 2 summarizes the assignments of the Raman bands for the $LiCF_3SO_3$ salt [18].

The study of ionic interaction of polymeric electrolytes is usually performed using the $\nu(SO_3)$ and $\delta_s(CF_3)$ modes [9,11,18–21]. These bands are chosen because they are associated with totally symmetric and non-degenerated vibration modes (A_1). Moreover, they are more sensitive to the salt addition and they provide the highest intensity in the electrolyte spectra. Therefore, the band separation in individual peaks can be related to different $CF_3SO_3^-$ anion associations. In this work we focus our attention on the behavior of the $\nu(SO_3)$ mode, since it was shown to be more sensitive to the different kinds of ionic aggregate.

Fig. 4 shows the Raman spectra of pure PDXL and $LiCF_3SO_3$ salt, as well as that of four different polymer electrolyte compositions, in the region of the $\nu(SO_3)$ mode. Line shape analysis is performed keeping the pure polymer peaks and adding the anion peaks. For the lowest salt concentration (2 wt%) the $\nu(SO_3)$ band may be fitted by a single Lorentzian line centered at (1031 ± 1) cm^{-1}. When the concentration is increased from 2 up to 58 wt%, the addition of other Lorentzian lines is necessary to perform the $\nu(SO_3)$ fitting. Table 3 summarizes the fitting parameters obtained for the $\nu(SO_3)$ band for samples with increasing concentrations of $LiCF_3SO_3$. It should be noted (Table 3) that each Lorentzian line is kept at both fixed frequency and linewidth when the next one is introduced [3].

Several authors have studied polymeric electrolytes by Raman spectroscopy using salts with $CF_3SO_3^-$ anion [9,11,18–21]. Their results partially support the assignment of the frequencies observed in the present work to the different ionic species. The Lorentzian line at 1031cm^{-1} is assigned to either free ions or solvent-separated ionic pairs, and the line at 1050cm^{-1} is associated to the positive triplets $[Li_2CF_3SO_3]^+$.

The high resolution of our measurements and the careful analysis of the lineshape allowed the observation of two peaks, at 1038 and 1043 cm^{-1}, which were not reported previously (see, for instance, Refs. [11,19]). The peaks at 1038 and 1043 cm^{-1} might be associated with the ionic pairs and negative triplet $[Li(CF_3SO_3)_2]^-$, respectively.

Table 3
Fitting parameters for the $\nu(SO_3)$ band of the PDXL/$LiCF_3SO_3$ system

w/w (%)	2		5		12		22		30		46		58	
Freq.	ν	$\Delta\nu$	ν	$\Delta\nu$	ν	$\Delta\nu$	ν	$\Delta\nu$	ν	$\Delta\nu$	ν	$\Delta\nu$	ν	$\Delta\nu$
(cm^{-1})	1031	10.4	1031	10.4	1031	10.4	1031	10.4	1031	10.4	1031	10.4	1031	10.4
			1038	8.4	1038	8.4	1038	8.4	1039	8.4	1038	8.4	1038	8.4
					1043	9.4	1043	9.4	1044	9.4	1043	9.4	1043	9.4
							1049	16.4	1052	16.4	1050	16.4	1051	16.4
									1063	7.0	1063	7.0	1063	7.0

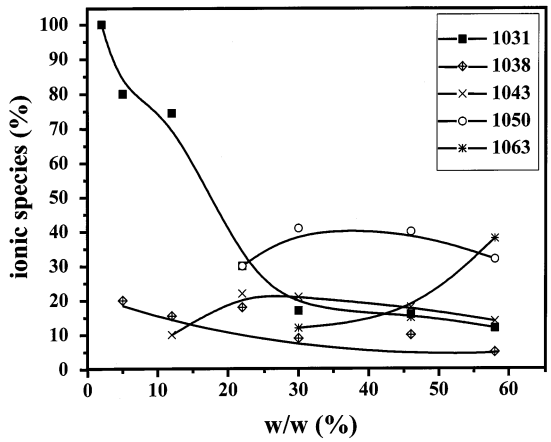

Fig. 5. Result of the band shape analysis of the $\nu(SO_3)$ mode as a function of salt concentration.

The peak at 1063 cm^{-1} is narrower than those at 1038 and 1043 cm^{-1}, and is present only in the spectra of very concentrated samples (46 and 58 wt%). As already discussed the X-ray diffractograms of these samples show a particular crystalline structure associated with the formation of a crystalline complex $PDXL_3/LiCF_3SO_3$ (58 wt% corresponds to $n=3$). Therefore, we assign the line at 1063 cm^{-1} to the $\nu(SO_3)$ mode in the complex.

PEO is known for its ability to form crystalline complexes with several salts, such as NaI, NASCN, $LiCF_3SO_3$ and $LIN(CF_3SO_2)_2$, having 3:1 stoichiometry [9]. These PEO complexes retain the helical conformation of PEO, but the cation is coordinated to oxygen atoms of the polymer chain, and also to the anionic species. The helical conformation of PDXL may allow

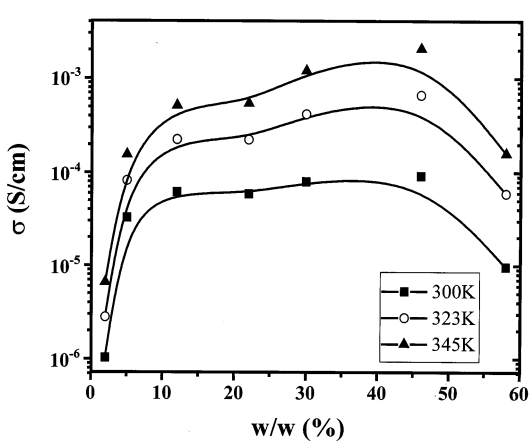

Fig. 6. Conductivity isotherms for $PDXL/LiCF_3SO_3$ systems as a function of salt concentration. The measurement temperatures are indicated in the figure. The solid lines are only guides for the eyes.

the formation of a complex, which involves the anion coordination with a stoichiometry 3:1, similar to that of the PEO systems mentioned.

Fig. 5 shows the relative area for each Lorentzian line obtained from the fitting of the $\nu(SO_3)$ mode as a function of salt concentration. The percentage of each ionic species, plotted in the Y axis, is calculated from the ratio of each peak area divided by the total area of the band. Two very interesting observations can be made based on Fig. 5: (i) the free anion proportion decreases abruptly in dilute solutions; and (ii) each superior aggregated species appears when the previous species approaches a saturated concentration. The relative area of the line assigned to the crystalline complex becomes significant at the two highest concentrations (46 and 58 wt%).

3.3. Ionic conductivity

Fig. 6 shows the total ionic conductivity obtained at three different temperatures for each salt composition. A pronounced increase of almost two orders of magnitude occurs when the salt concentration is raised from 2 to 12 wt%. Over this concentration range a "plateau" of conductivity occurs up to 46 wt% salt at 300 K. The two highest temperature isotherms, at 323 and 345 K, show an increase in conductivity between 22 and 46 wt% salt. The most concentrated sample, 58 wt%, ($n=3$) shows a significant decrease in conductivity for the three temperature isotherms.

The increase in conductivity up to 12 wt% coincides with the pronounced decrease in free anion concentration observed in Fig. 5. This behavior supports the conclusion that the charged ionic aggregates contribute significantly to ionic transport. Between 12 and 46 wt% the concentration of ion triplets, and especially of the positive triplet, guarantees the high level of conductivity. The positive triplet is present in a proportion of 40% in relation to the sum of the other species between 12 and 46 wt% (Fig. 5). The effective formation of a polymer/salt complex certainly contributes to the decrease in ionic conductivity at 58 wt%.

4. Conclusions

Electrolytes based on $PDXL/LiCF_3SO_3$ have been studied in the range of 2–58 wt% salt concentration. DSC results show a linear increase in T_g between 12 and 58 wt% of salt. The 2 and 5 wt% electrolytes are significantly crystalline and present T_g transitions broader than those of the most concentrated samples, which is probably related to amorphous heterogeneities and constraint.

The three most dilute electrolyte samples, 2, 5 and 12 wt%, exhibit a crystalline structure similar to that of

pure PDXL, and their conductivities increase between 10^{-6} (2 wt%) and 6×10^{-5} cm^{-1} (12 wt%) at 300 K. From 12 to 46 wt% at 300 K, the conductivity remains approximately constant at $(6–7) \times 10^{-5}$ S cm^{-1}.

The $\nu(SO_3)$ Raman band was fitted with up to five Lorentzian lines: (1) at 1031 cm^{-1}, assigned to free anions; (2) at 1038 cm^{-1}, assigned to the ionic pairs; (3) at 1043 cm^{-1}, assigned to negative triplets; (4) at 1050 cm^{-1}, assigned to positive triplets; and (5) at 1063 cm^{-1}, assigned to the crystalline complex. The appearance of each superior aggregated species occurs when the concentration of the last one saturates (Fig. 5).

The X-ray diffractogram of the 58 wt% sample presents narrow Bragg peaks, and the Raman spectrum exhibits an intense peak at 1063 cm^{-1}, indicating the formation of a $PDXL_3/LiCF_3SO_3$ complex similar to that of the most studied system, $PEO_3/LiCF_3SO_3$. For this sample the electrical conductivity decreases by one order of magnitude in relation to the "plateau" observed for the 12–46 wt% salt electrolytes, which is a consequence of the increase in T_g and of the formation of the crystalline complex.

Acknowledgements

This work was supported by the Brazilian agencies CNPq and CAPES. The PDXL sample was prepared in the Institut National Polytechnique of Grenoble, France. G.G.S. wishes to thank J.-Y. Sanchez for the supervision of the synthesis work.

References

[1] G. Goulart, S. Sylla, J.Y. Sanchez, M. Armand, in: B. Scrosati (Ed.), Proceedings of the Second International Symposium on Polymer Electrolytes (ISPE2), Elsevier, London, 1990, p. 99.
[2] G. Goulart, J.Y. Sanchez, M. Armand, Electrochim. Acta 37 (1992) 1589.
[3] R.A. Silva, G. Goulart Silva, M. Pimenta, Appl. Phys. Lett. 67 (1995) 3352.
[4] M. Alamgir, R.D. Moulton, K.M. Abraham, Electrochim. Acta 36 (1991) 773.
[5] F.M. Gray, Solid Polymer Electrolytes, VCH, Cambridge, 1991.
[6] M. Armand, Solid State Ionics 69 (1994) 309.
[7] W.H. Meyer, Adv. Mater. 10 (1998) 439.
[8] H.A. Allcock, S.J.M. O'Connor, D.L. Olmeijer, M.E. Napierala, C.G. Cameron, Macromolecules 29 (1996) 7544.
[9] F.M. Gray, Polymer Electrolytes, RSC Materials Monographs, Cambridge, 1997.
[10] M. Armand, W. Gorecki, R. Andreani, in: B. Scrosati (Ed.), Proceedings of the Second International Symposium on Polymer Electrolytes (ISPE2), Elsevier, London, 1990.
[11] L.M. Torrel, S. Schantz, in: J.R. MacCallum, C.A. Vincent (Eds.), Polymer Electrolyte Reviews, vol. 2, Elsevier, London, 1989.
[12] S. Sasaki, Y. Takahashi, H. Tadokoro, J. Polym. Sci.: Polym. Phys. Ed. 10 (1972) 2363.
[13] H. Tadokoro, Y. Chatani, T. Yoshihara, S. Tahara, S. Murahashi, Makromol. Chem. 73 (1964) 109.
[14] R. French, S. Chintapalli, P.G. Bruce, C.A. Vincent, Chem. Commun. (1997) 157.
[15] P. Archambault, R.E. Prud'Homme, J. Polym. Sci.: Polym. Phys. Ed. 18 (1980) 35.
[16] G. Goulart Silva, N.H.T. Lemes, C.N. Polo da Fonseca, M.-A. de Paoli, Solid State Ionics 93 (1997) 105.
[17] A. Vallée, S. Besner, J. Prud'Homme, Electrochim. Acta 37 (1992) 1579.
[18] B. Sander, J. Tübke, S. Wartewig, S. Shashkov, Solid State Ionics 83 (1996) 87.
[19] A. Ferry, J. Phys. Chem. B 101 (1997) 150.
[20] A. Ferry, G Orädd, P. Jacobsson, J. Chem. Phys. 108 (1998) 7426.
[21] R. Frech, S. Chintapalli, P.G. Bruce, C.A. Vincent, Macromolecules 32 (1999) 808.